

Spontaneous Self-Assembly of Transcription Factor Based Gene Regulation Networks

D. Balcan¹, A. Kabakçioğlu², M. Mungan^{3,4}, and A. Erzan^{1,4}

¹*Department of Physics, Faculty of Sciences and Letters*

Istanbul Technical University, Maslak 34469, Istanbul, Turkey

²*Department of Physics, Faculty of Arts and Sciences, Koc University, 34450 Sariyer Istanbul, Turkey*

³*Department of Physics, Faculty of Arts and Sciences*

Bogaziçi University, 34342 Bebek Istanbul, Turkey and

⁴*Gürsey Institute, P.O.B. 6, Çengelköy, 34680 Istanbul, Turkey*

(Dated: November 6, 2018)

We model the transcription factor based regulation network of yeast using a content-based network model that mimicks the recognition of binding motifs on the regulatory regions of the genes. We are thereby able to faithfully reproduce many of the topological features of the gene regulatory network of yeast once the parameters of the yeast genome, in particular the distribution of information coded by the “binding sequences” within the promoter regions is provided as input. The length distribution for the promoter regions is fixed by comparing the k-core analysis of the model network with that of yeast. Our results strongly point to the possibility that the observed topological features are generic to networks formed via sequence-matching between random strings obeying certain length distributions.

I. INTRODUCTION

Development of new experimental techniques, such as DNA microarrays, in the late 1990’s [1, 2] made a huge impact on cell biology research. Such experiments generated a flood of expression data for several well-studied single-cell species for which we now have an almost complete list of not only the genes, but also the interactions between them. A cell is able to survive, grow and replicate due to the collective actions of its genes. The adaptation and robustness of its activities in a constantly changing environment is maintained by the complex network of interactions between the genes.

The regulation of gene expression in a cell relies to a major extent on dedicated proteins called transcription factors (TFs). [3] These proteins come with a structure suited to recognize and bind the DNA at specific locations called binding sites. The binding affinity of a TF on a certain DNA segment is determined by the base sequence at the location. Each TF preferentially binds certain regulatory sequences or binding motifs, within the promoter regions (PRs) responsible for the regulation of the gene. In the case of yeast, *Saccharomyces cerevisiae*, a list of the binding motifs for more than 100 TFs has recently been provided. [4, 5] It was also reported [5] that the TF binding sites are located with high probability within a window of several hundred bases upstream of the transcription activation site (preceding the start codon of the gene), although longer-distance action is also possible. In fact, the existence of a high-affinity binding motif in a promoter region is a necessary but not sufficient condition for TF-based expression regulation [5]. Moreover, especially in eukaryotic cells, gene regulation relies on the simultaneous action of multiple TFs.

We argue that the global features of the gene regulation network depend very little on such details and are largely determined by the distribution of the amount of shared information or content, that is required for the

establishment of regulatory interactions. It may be conjectured that information sharing and its distribution is the basic organizing principle which is responsible for the universality of the degree distribution of gene regulatory networks across diverse species [6].

In this paper we propose to model the transcription regulation network of yeast using the ideas of the content-based model we introduced earlier [7, 8]. We are able to faithfully reproduce all the topological aspects of the gene regulatory network of yeast when the parameters of the yeast genome, in particular the distribution of information coded by the “binding sequences” of the regulatory segments, are given as input. We compare the ensemble of the resulting model networks with the data on the yeast regulatory network available in different databases.

Gene regulatory networks can be naturally described as a directed graph where the nodes are the genes. A directed edge from node A to node B implies that the transcription factor produced by gene A regulates the activity of gene B. Since the edges are directed, one distinguishes the in-degree (the number of incoming edges), the out-degree (number of outgoing edges) and the total degree of a node, each with their own (possibly distinct) probability distributions. These distributions serve as distinguishing features of the network which a realistic model is expected to reproduce. Further structural aspects of these networks are probed by measures such as the clustering coefficient $C(k)$ [9, 10], the degree-degree correlation between connected vertices [11], the “rich-club coefficient” [12, 13], or the k -core decomposition [14] recently employed to predict new interactions in various biological systems [15, 16, 17, 18, 19].

This report is organized as follows: In Section II we introduce our model, which we compare with the experimentally determined yeast regulatory network in III. A discussion is provided in Section IV, while Section V outlines our methods.

II. THE MODEL

The nodes of our model network correspond to genes. We differentiate between genes which code for a Transcription Factor (TF) and those which do not. All genes are assumed to be possible targets of regulation by one or more TFs. Each node has a sequence associated with it, representing the promoter region (PR) through which the corresponding gene may be regulated. We pick a given percentage of nodes (around 5%, see Table I) at random, to represent TF-producing genes. With each TF-producing node/gene we also associate a second sequence, which stands for the binding motif, which the TF recognizes and binds in the promoter region of another gene.

We represent both the binding motifs and the PRs as random binary sequences of variable length. The mechanism for establishing connections between nodes of the gene regulatory network is given by a string matching condition [7, 8], between the binding motifs of the TF's and all possible uninterrupted subsequences of the PRs. The (directed) network of regulatory gene interactions is then obtained by connecting each TF-producing node A to all those nodes B, B', B'' ... whose PRs contain the binding motif associated with node A. The amount of information coded in these randomly generated binding motifs and promoter regions constitutes the essential ingredient of our model and dictates the overall topology of the resultant networks.

Experimentally determined TF binding motifs are typically short sequences with a narrow length distribution, since a TF selectively binds 5-10 bases and not much more. A single TF can bind a range of similar motifs, and the relative frequencies of the four bases at each position within the motif contribute to the information exchanged in the binding process. The promoter regions (PRs) which lie in the intergenic portions of the genome are typically longer and may accommodate several binding motifs (as shown in Fig. 1) to allow graded and/or combinatorial regulation [3, 5].

The bitwise length distribution of the model binding motifs was derived from the yeast data provided by Harbison et al. in [5]. The motifs were reported [5] as letter sequences comprising the symbols for the four bases {ATGC}, or the symbols {YMKRSW} for incompletely specified bases, with the corresponding lower case letters indicating a lower confidence level. In order to account for such variations in the information content of the motifs, we assigned two bits to each of the letters {ACTG} appearing in the motif, signifying a high information content at that position, and one bit otherwise. The length of the bit sequence obtained in this way roughly corresponds to the amount of shared information, measured by the Shannon entropy [20], required for the binding of the TF. Performing this calculation for each TF in [5], we obtain the length distribution shown in Fig. 2.

In choosing the length distribution of the promoter regions, about which less is known, we are guided by the

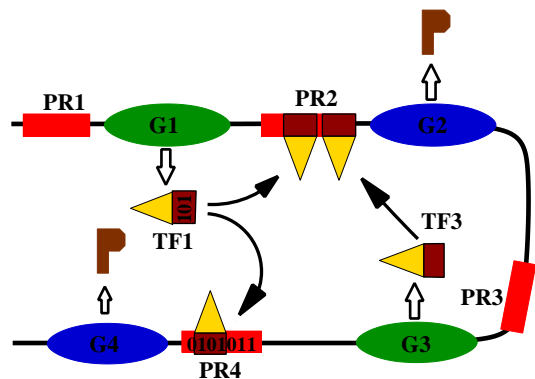


FIG. 1: The mechanism of interaction between the genes as envisaged in our model. The genes are indicated by ellipses (green if TF-coding, blue otherwise), the transcription factors by triangles with the associated binding motif in the box underneath. Non-TF proteins are symbolized by the “P” shape, and the promoter regions (PR) upstream of each gene are shown as red boxes. Binding occurs if the binding motif matches a subsequence in the PR, as is the case here at PR4. PRs in the model are typically much longer than depicted here.

finding [5] that most of the probability for encountering a TF binding site is contained within a window of 250 base pairs (bps) located approximately 100 bps upstream of a gene. The PR length distribution that we adopt within this range decays with a power law $p(l) \propto l^{-1-\mu}$, with $0 \leq \mu \leq 2$ after the findings of Almirantis and Provata [21] for the lengths of intergenic regions. We also assign a minimum length chosen to coincide with the peak of the motif-length distribution shown in Fig. 2. Note that the 250 bps window does not double as we move from the 4 letter alphabet to a binary one, because the matching probabilities and the total number of positions at which the TFs may bind are required to remain invariant under this transformation.

The value of μ remains as the only adjustable parameter in our model, and is determined by comparing the k -core decomposition of the gene regulatory network of yeast as extracted from experimental data (Table I) with our content-based network model, as explained in the Methods section.

The collection of such model networks forms an ensemble whose features are a direct consequence of the string-matching mechanism and the length distributions. Clearly, each realization of the model will result in a different collection of random PRs and binding motifs, and hence a somewhat different network. These features turn out to be strikingly distinct from those encountered in random [22] or scale-free [23] networks. We show below that the “signatures” of this ensemble are shared by the yeast regulatory network.

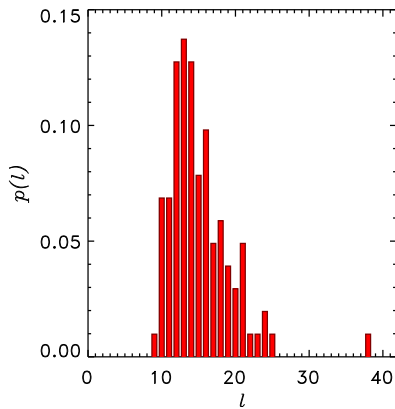


FIG. 2: Distribution of the amount of bitwise information coded by each regulatory sequence recognized and bound by the 102 TFs in the yeast genome (compiled from the recently published data by Harbison et al. [5]). This distribution is adopted as the length distribution of the random regulatory sequences (“binding motifs”) in our model.

III. RESULTS

Our purpose here is to show that the experimentally determined features of the yeast regulation network follow closely those typical of the ensemble defined by our model. The topological features we will focus on are the following:

1. **degree distribution** (in-, out-, and total): the distribution of the number of connections of the nodes in a network.
2. **clustering coefficient**: the modularity of the network.
3. **degree-degree correlations**: average degree of the neighbors of a node with degree k .
4. **“rich-club” coefficient**: a measure of the relative connectivity among nodes whose degree is higher than a given number.
5. **k -core structure**: the hierarchical structuring in the network

The precise definition of these quantities is given in the Methods section.

Here we will report the comparison of our results with the most recent Yeasttract [24] data. Analogous comparisons with each of the data sources listed in Table I yield similar results (see Supplementary Material) showing that our conclusions are consistent with all the different data sets available.

In order to compare our results with the available data we generate an ensemble of realizations, with an average

TABLE I: The number of interacting genes, TFs, and interacting pairs that appear in the yeast regulatory network as obtained from different sources.

Source	Genes	TFs	Interacting Pairs
Fraenkel Lab ^a	2884	102	6441
Yeasttract ^b	4252	146	12530
Luscombe et al. ^c	3459	142	7071
Kirdar et al. ^d	3763	180	9135

^ahttp://fraenkel.mit.edu/Harbison/release_v24/bound_by_factor/

^b<http://www.yeasttract.com>

^c<http://sandy.topnet.gersteinlab.org/index2.html>

^dprivate communication

of $N_G = 6000$ genes in total, 4167 of which contribute to the network on the average. Out of these, 202 (making up % 4.8 of the genes) are TF-coding genes, taking part in a total of 14365 interactions, again on the average. The corresponding values for the yeast regulatory networks reported in the publicly available data bases are given in Table I.

The total degree distribution is obtained by ignoring the directionality of the interactions and is different from the superposition of in- and out-degree distributions. In Fig. 3a, Yeasttract data for the degree distribution is shown on top of a scatter plot obtained by superposing the results from 100 artificial model genomes independently generated according to the rules described in Section II. In Fig. 3b, we exhibit the in-degree distribution obtained from the Yeasttract data, and the corresponding scatter plot.

The out-degree distribution of the yeast and model networks exhibits a rather large scatter of points due to the relatively small number of TFs. Comparing with the scatter plot obtained from 100 realizations, we find again that the actual yeast data falls within the boundaries set by the model ensemble (Fig. 3c).

In Fig. 4, we report the three topological coefficients, the clustering coefficient, the degree-degree correlation and the “rich-club” coefficient, that go beyond degree-distributions in characterizing the network. The agreement is extremely good; in particular, the shoulder observed in the “rich-club” coefficient in Fig. 4(c), a feature common to both gene-regulation and protein-protein interaction networks [11], is captured accurately in our model.

The agreement observed with the Yeasttract data is not source-specific, as can be seen from a comparison of the topological properties of our model networks, with those obtained from the different sources listed in Table I. (see Supplement)

Finally, in Fig. 5, left, the k -core analysis of the model network is shown, which should be compared with that of the Yeasttract data on the right. The k -core analysis provides a much more stringent characterization of a network than the other single topological features considered above. To give an idea of the sensitivity of the k -core analysis to the structure of the network, let us

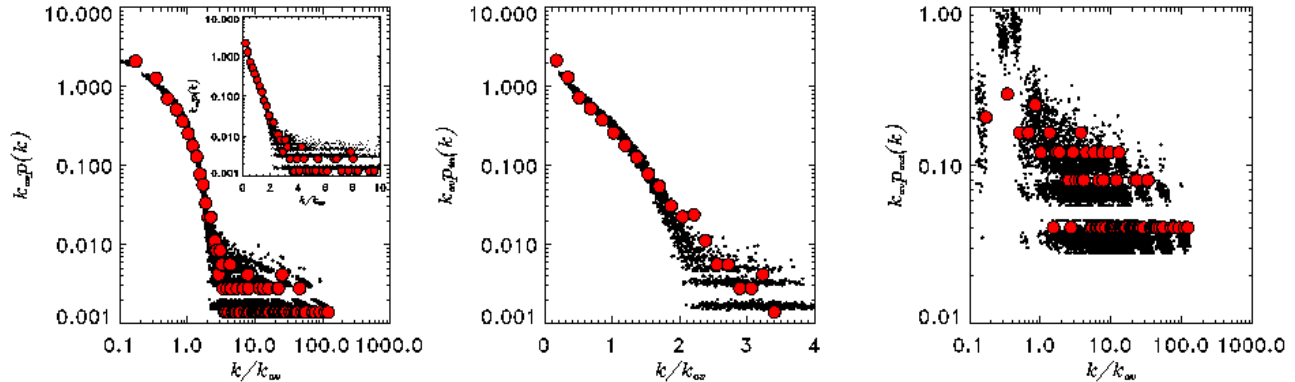


FIG. 3: Degree distributions extracted from the Yeastract [24] data (red circles), superposed on the corresponding degree distributions of 100 realizations of the model network (black dots). From left to right, a) The total degree distribution with an inset showing a log-linear plot for $k/k_{av} \leq 10$, where one may observe that both the model and the data points almost fall on a straight line. b) The in-degree distribution plotted on a semi-logarithmic scale. c) The out-degree distribution plotted on a log-log scale. The axes are scaled by the average total degree in order to factor out sample-to-sample fluctuations in the network size.

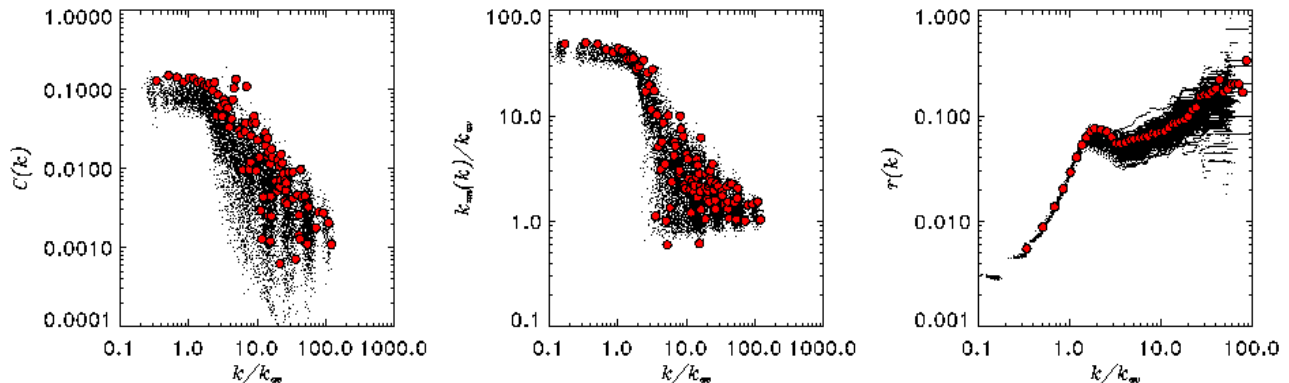


FIG. 4: Comparison of a) the clustering coefficient $c(k)$, b) the degree-degree correlations between neighboring nodes $k_{nn}(k)$, and c) the rich-club coefficient $r(k)$, from left to right, for 100 realizations of the model (black dots) and the Yeastract data (red circles).

point out that, under a shuffling of the edges of the network keeping the degree of each node fixed, the typical value of the maximum number of k -cores, k_{max} , becomes

29 rather than 9 as observed in both the real yeast regulatory network and the model (see Supplement).

IV. DISCUSSION

The close structural similarity between the model and the real yeast regulatory network, with respect to a diverse set of criteria, shows that they are part of the same statistical ensemble of networks, formed by random strings connected by the sequence matching rule.

The sequence matching rule could more generally be viewed as an information-theoretical constraint, where the interaction between two genes requires the fulfillment

of a set of conditions which we symbolically represent as the matching of two random sequences. The more stringent the prerequisites of the interaction, the longer is the random “binding motif” that is to be matched. The length of the PR establishes the size of the phase space in which the motif is to be sought. The properties of the network are then determined by the distributions obeyed by the lengths of the binding motifs as well as the promoting regions.

Interpreted within this information-theoretical frame-

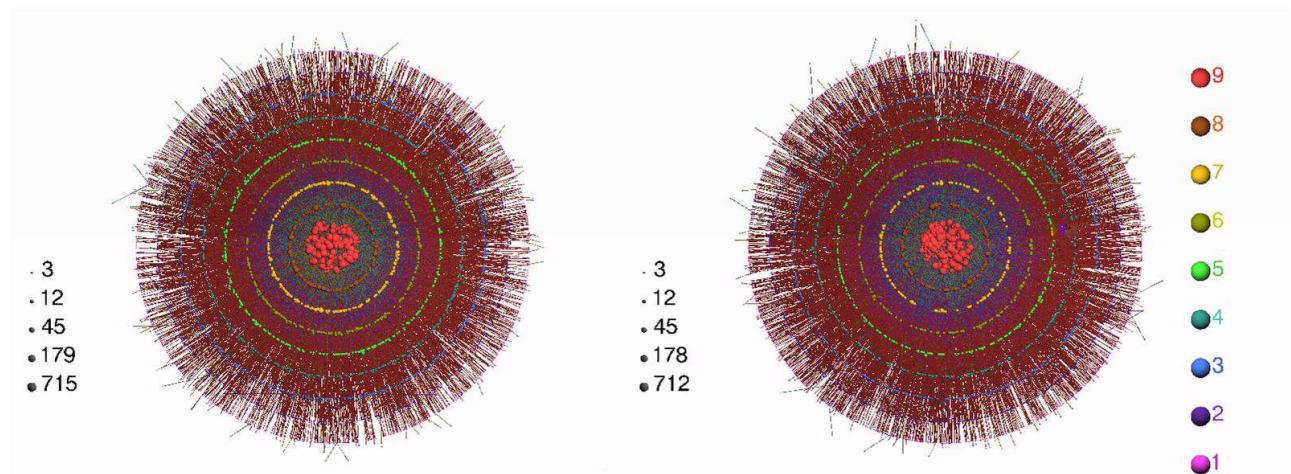


FIG. 5: Left: The k -core decomposition of a single realization of our model network obtained with the visualization tool lanet-vi [25]. The length distribution exponent of the PR sequences has been adjusted to $\mu = 0.1$ to optimize the similarity with the k -core distribution of the Yeastract data (Right). Dots represent the nodes of the network, while edges between nodes depict connections. Nodes belonging to different k -shells are indicated by different colors (on the right hand side) and are arranged around concentric circles, whose average radius decreases with k . In particular, a node of a given shell is placed just inside (outside) the corresponding circle, if it is preferentially connected to lower (higher) k -shells. The size of dots indicate the degree of the respective nodes; see legends to the left of the figures.

work, our model has sufficient generality to accommodate other interactions based on lock-and-key mechanisms, such as protein networks, where the interactions are dictated by certain steric and chemical conditions.

The topological features of the networks investigated here and shown to be shared by the yeast regulatory network strongly point to the possibility that these networks did not have to be assembled from scratch, but rather emerged spontaneously, given any sufficiently long linear code. This proposition by no means minimizes the role of evolutionary pressures on such networks; instead,

it suggests that a network with essentially the current topology could have provided a starting point for further fine-tuning. As a case in point, it has recently been demonstrated that evolution under duplication and divergence [26] may leave the topological features of such networks essentially invariant [27]. Such a perspective will hopefully bring us a step closer to envisioning how complex structures may have come into existence, by shifting some of the load from the shoulders of evolution onto the laws of probability.

V. METHODS

The degree k of a node is the number of edges connected to it. When the graph is directed, one distinguishes in-, out-, and total-degrees of a node, with their corresponding distributions. In the measures below we have ignored the directionality of the network.

The clustering coefficient is given by the formula:

$$C_i = \frac{\Delta_i}{k_i(k_i - 1)/2},$$

where Δ_i is the number of triangles that contain node i . The quantity $C(k)$ plotted in Fig. 4 is the average of C_i over the nodes with degree k .

The degree-degree correlation function $k_{nn}(k)$ is

$$k_{nn}(k) = \sum_{k'} k' p(k'|k),$$

where $p(k'|k)$ is the conditional probability that a node with degree k is connected to a node with degree k' .

The “rich-club” coefficient [12, 13] $r(k)$ is the total number $e_{>k}$ of edges connecting nodes with degree greater than k , normalized by the maximum possible number of such connections,

$$r(k) = \frac{2e_{>k}}{N_{>k}(N_{>k} - 1)},$$

where $N_{>k}$ is the total number of nodes with degree greater than k .

The k -core decomposition performs a successive pruning on the least connected vertices of a network [14]. At each step one removes all nodes with a degree less than k along with their edges and continues in this manner until all nodes have at least degree k . The remaining nodes constitute the k core. Next, k is incremented by one, and the process is repeated until no nodes are left.

The k -shell is defined as the set of nodes that belong to the k -core, but not the $(k + 1)$ -core.

Once the shape of the TF length distribution, the width of the PR region, as well as the functional form of its distribution have been fixed through the available biological data, the only remaining adjustable parameter in our model is the exponent μ of the power law distribution of PR lengths, $p(l) \propto l^{-1-\mu}$. The k -core decomposition turns out to provide the most detailed and stringent topological characterization of the network, with both the total number of shells, and the distribution of the nodes over the shells, being contained in the k -core plots (see Fig.5). The k -core plots also incorporate such qualitative features as inter- and intra-shell connectivity. We have therefore used qualitative and quantitative comparison of the k -core plots for the Yeasttract and the model network to determine μ . The best agreement was obtained for $\mu = 0.1$. Once μ has been fixed, no further adjustment is needed in order to obtain the extremely close matching that is found between the degree distributions, clustering coefficients, degree correlations and the rich-club coefficient, as displayed in Figs. 3 and 4.

We cannot rule out the possibility of obtaining similar agreement between our model and the real genomic network with respect to the features considered here, for a different choice of the functional form of the length distribution for the PR sequences, once more determining an adjustable parameter from a comparison of the k -core plots. However, the present choice seems to be the only reasonable one within the physical constraints and the available information.

VI. ACKNOWLEDGMENTS

We would like to thank Betül Kırdar and Beste Kımkoğlu for the use of their data and useful discussions. It is a pleasure to thank Alessandro Vespignani and Ignacio Alvarez-Hamelin for bringing k -core analysis to our attention, and for the use of their web-based k -core analysis tool. AE would like to thank Tamás Vicsek and András Czırók for a useful discussion and is grateful for partial support from the Turkish Academy of Sciences.

-
- [1] Lockhart, D.J., Winzeler, E.A. (1995) *Nature* **405**, 827-36.
 - [2] Spellman, P.T., Sherlock, G., Zhang, M.Q., Iyer, V.R., Anders, K., Eisen, M.B., Brown, P.O., Botstein, D., Futcher, B. (1998) *Molecular Biology of the Cell* **9**, 3273-3297.
 - [3] Alberts, B., Johnson, A., Lewis, J., Raff, M., Roberts, K., Walter, P. (2002) in *Molecular Biology of the Cell*. Chapter 9. (Garland Science, N.Y.).
 - [4] Lee, T.I., Rinaldi, N.J., Robert, F., Odom, D.T., Bar-Joseph, Z., Gerber, G.K., Hannett, N.M., Harbison, C.T., Thompson, C.M., Simon, I. et al. (2002) *Science*, **298**, 799-804.
 - [5] Harbison, C.T., Gordon, D.B., Lee, T.I., Rinaldi, N.J., Macisaac, K.D., Danford, T.W., Hannett, N.M., Tagne, J.B., Reynolds, D.B., Yoo, J., et al. (2004) *Nature* **431**, 99-104.
 - [6] Bergmann, S., Ihmels, J., Barkai, N. (2004) *PloS Biol.* **2**, 85-93.
 - [7] Balcan, D., Erzan, A. (2004) *Eur. Phys. J. B* **38**, 253.
 - [8] Mungan, M., Kabakcioglu, A., Balcan, D., Erzan, A. (2005) *J. Phys. A* **38** (44), 9599-9620.
 - [9] Dorogovstev, S.N., Mendes, J.F.F. (2002) *Adv. Phys.* **51**, 1079-1187.
 - [10] Watts, D.J. & Strogatz, S.H. (1998) *Nature* (London) **393**, 440-442.
 - [11] Colizza, V., Flammini, A., Maritan, A., Vespignani, A. (2005) *Physica A* **352**, 1-27.
 - [12] Zhou, S. & Mondragon, R.J. (2004) *IEEE Commun. Lett.* **8**, 180-182.
 - [13] Colizza, V., Flammini, A., Serrano, M.A. & Vespignani, A. (2006) *Nature Physics* **2**, 110-115.
 - [14] Bollobas, B., (1998) *Modern Graph Theory* (Springer Verlag, New York).
 - [15] Tong, A.H.Y., Drees, B., Nardelli, G., Bader, G.D., Brannetti, B., Castagnoli, L., Evangelista, M., Ferracuti, S., Nelson, B., Paoluzi, S. et al. (2002) *Science* **295**, 321-324.
 - [16] Bader, G.D. & Hogue, C.W.V. (2002) *Nature Biotechnology* **20**, 991-997.
 - [17] Bader, G.D. & Hogue, C.W.V. (2003) *BMC Bioinformatics*, **4**(2)
 - [18] Altaf-Ul-Amin, M., Nishikata, K., Koma, T., Miyasato, T., Shinbo, Y., Arifuzzaman, M., Wada, C., Maeda, M., Oshima, T., Mori, H. et al. (2003) *Genome Informatics*, **14**, 498-499.
 - [19] Wuchty, S. & Almaas, E. (2005) *Proteomics*, **5**(2), 444-449.
 - [20] Shannon, C. E., (1949) *Proc. IRE* **37**, 10-21.
 - [21] Almirantis, Y. and Provata, A. (1999) *J. Stat. Phys.* **97**, 233-262.
 - [22] Erdős, P. & Rényi, A., (1960) *Publ. Math. Inst. Hung. Acad. Sci.* **5**, 17-60.
 - [23] Jeong, H., Tombor, B., Albert, R., Oltvai, Z.N., Barabasi, A.-L. (2000) *Nature* **407**, 651-654; Albert, R., Jeong, H., Barabasi, A.-L., (1999) *Nature* **401**, 130-131.
 - [24] Teixeira, M.C., Monteiro, P., Jain, P., Tenreiro, S., Fernandes, A.R., Mira, N.P., Alenquer, M., Freitas, A.T., Oliveira, A.L., Correia, I. (2006) *Nucl. Acids Res.* **34**, D446-451.
 - [25] Alvarez-Hamelin, I., Dall'Asta, L., Barrat, L., Vespignani, A. Arxiv preprint cs.NI/0504107
 - [26] Wagner, A. (2001) *Mol. Bio. Evol.* **18**, 1283.
 - [27] Şengün, Y., Erzan, A. (2006) *Physica A* **365**, 446-462.
 - [28] Albert, R. and Barabasi, A.-L. (2002) *Rev. Mod. Phys.* **74**, 47-97.

Supplementary Material 1
Comparison with yeast data from different data bases

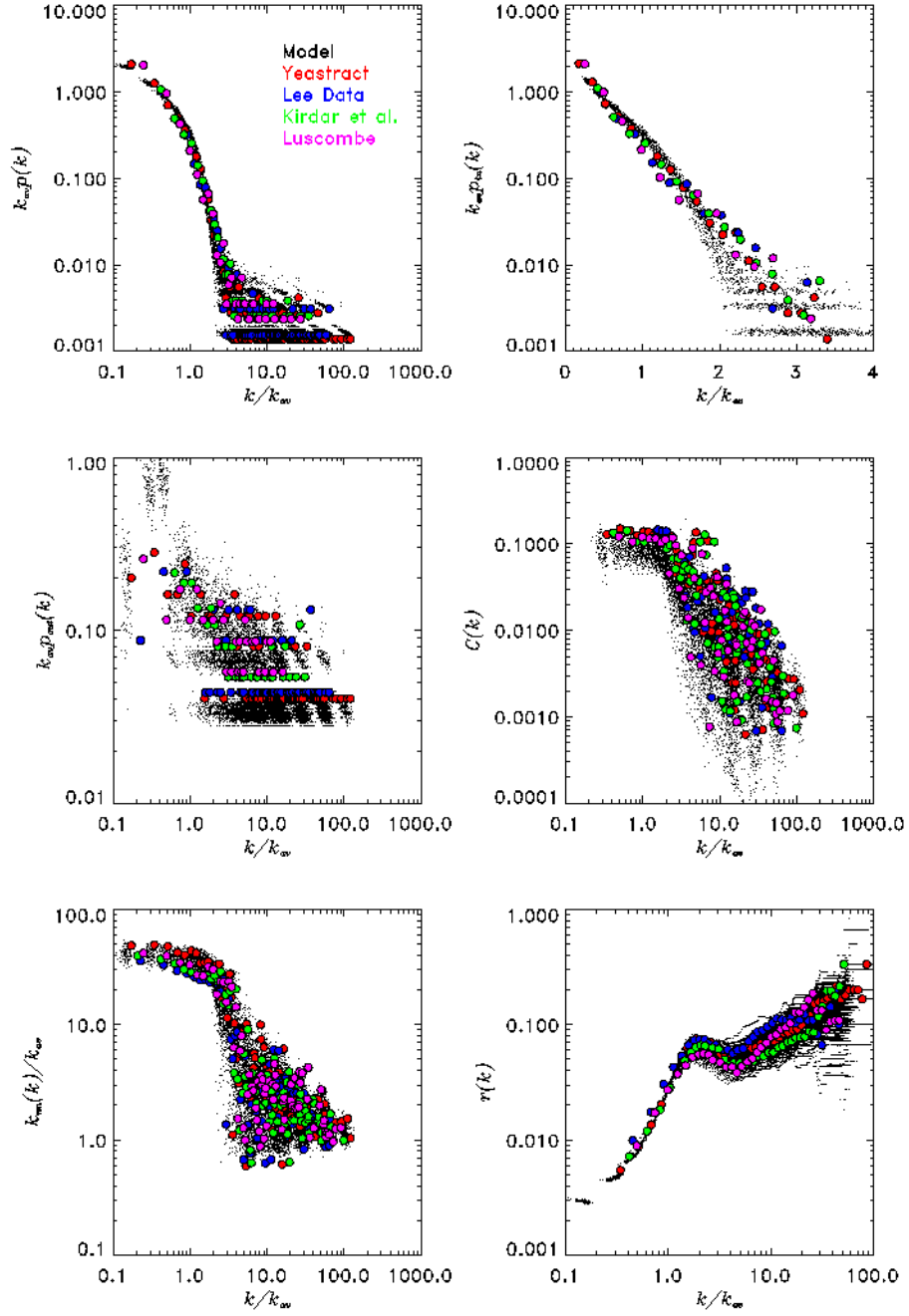


FIG. 6: The network statistics extracted from the sources listed in Table I superposed on the simulation results corresponding to 100 realizations of the model network (black dots). The agreement is extremely good with all of these sets of data, which almost completely cover, but do not exceed the phase space of our model. (Black, red, blue, green yellow and maroon correspond to the model, Yeabstract, Fraenkel Lab, Kirdar and Luscombe data respectively).

Supplementary Material 2

Comparison with Randomized Networks

To double check the significance of our other results, we also compared the clustering coefficients, the degree-degree correlations and the rich-club coefficients of the Yeastract data with those obtained after the randomly reconnecting the edges of the network while keeping the degree of each node fixed. In this process, the directionality of the bonds is ignored. The comparison of the topological coefficients of the randomized yeast and randomized model networks with that of the yeast network, as shown in Fig. (7), confirm that the observed agreement between the yeast and models networks is not spurious.

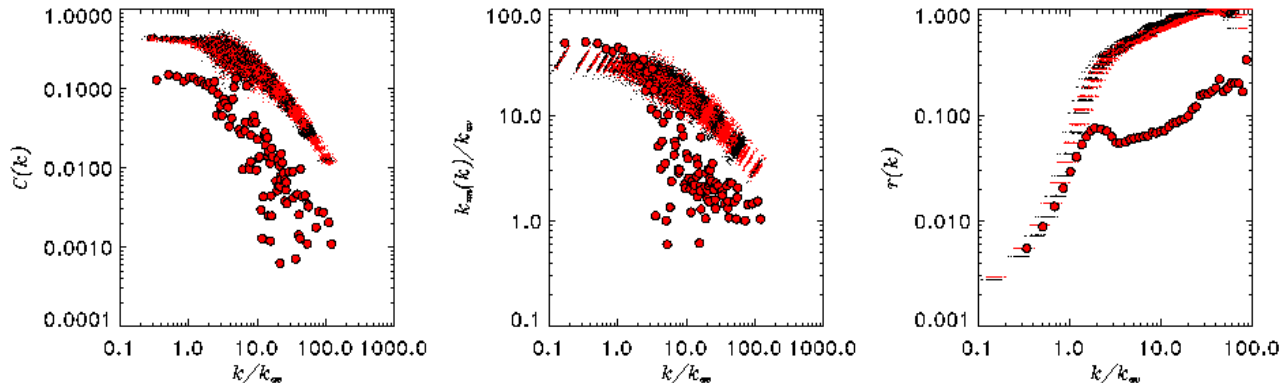


FIG. 7: a) The clustering coefficient, b) the degree-degree correlations between neighboring nodes, and c) the rich-club coefficient of Yeastract data (red circles) compared with the results for the same obtained by randomizing the Yeastract data (red dots) and randomizing a realization of the model network (black dots), keeping the degrees of the individual nodes, and thereby the degree distributions, fixed.

In Fig. 8 we display the effect of performing the same randomization procedure as described above, on the k -core plots. It is instructive to note that while in the yeast and model networks, a large fraction of connections is between nearby shells, the situation is reversed in the randomized networks, where there is a high degree of intra-shell connectivity as can be seen from Fig. 5.

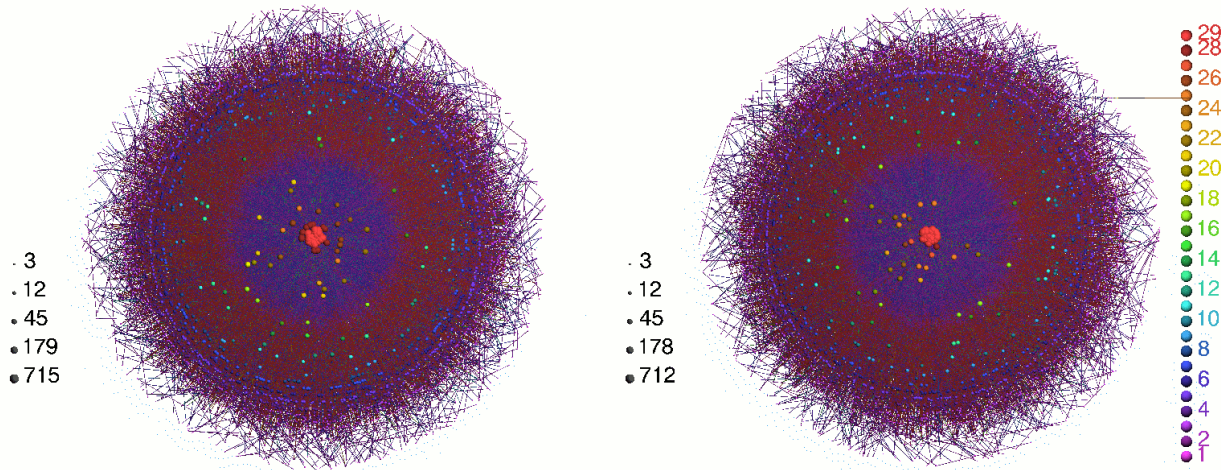


FIG. 8: The k -core analysis of the randomized versions of the model (left panel) and Yeastract (right panel) networks yield results that differ quantitatively and qualitatively from the originals. The number of shells have gone up to 29 from 9, and the much higher intra-shell rather than inter-shell connectivity (as can be seen by following the edges) indicates that the hierarchical nature of the yeast network, which is faithfully reproduced by the model, is destroyed by the randomization process.

Supplementary Material 3

The k -core structure of the Balcan-Erzan and Barabasi-Albert Networks

In Fig. 9 we show the k -core structure of the Balcan-Erzan [7] and Barabasi-Albert [28] network, as models for complex networks. Note the absence of well-defined hierarchical structures.

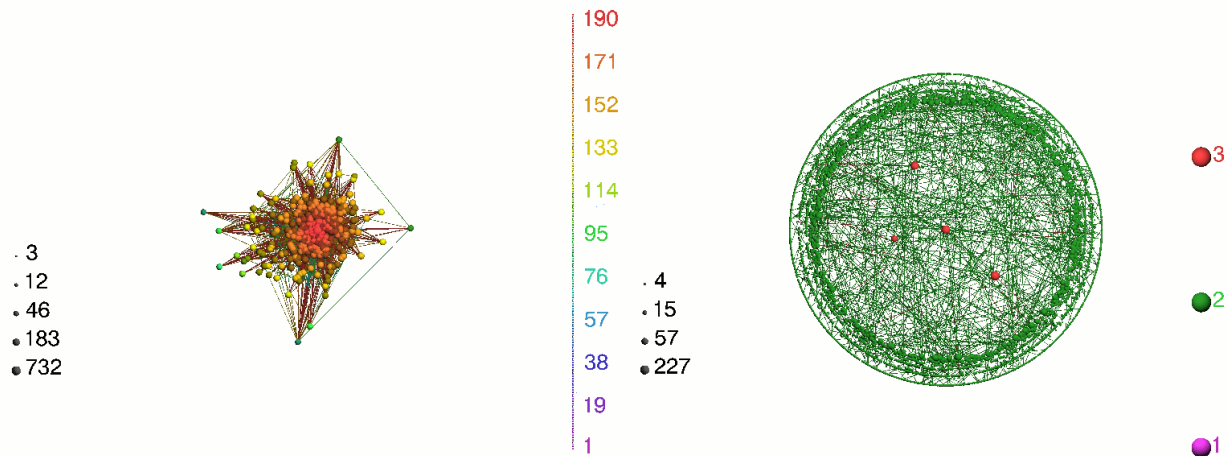


FIG. 9: The k -core analysis of the content-based network of Balcan and Erzan [7] (left panel) and the Barabasi-Albert (BA) model [28]. In the left panel, the total length of the single sequences associated with all of the nodes is $L = 15000$. The individual sequences obey the length distribution $p(l) \propto q^l$, with $q = 0.95$. The BA model network (right panel) has 5000 nodes, and is built by starting from a fully connected four-cluster and adding nodes with two edges at a time. In the k -core plot for the latter, only % 5 of the edges are shown for better visibility.

Supplementary Material 4

Ranking of overlapping sets of regulated genes and motif inclusion

We here report a statistical fact in support of the basic assumption underlying our model. The matching condition we employ dictates a certain correlation between the sets of regulated genes by each TF: if the binding motif of a TF (A) is embedded in that of a TF (B), then the set of genes $\{G_i\}_B$ regulated by TF_B in our model is a subset of $\{G_i\}_A$. A similar investigation of the yeast databases listed below reveals that the top 50% of the TF pairs related by the motif inclusion relation above, rank in the top 3% when all the TF pairs are listed according to the overlap of their $\{G_i\}$ sets. The actual ranking of the TF pairs obtained among all possible pairs of 102 TFs with known binding motifs is shown in Fig. 10.

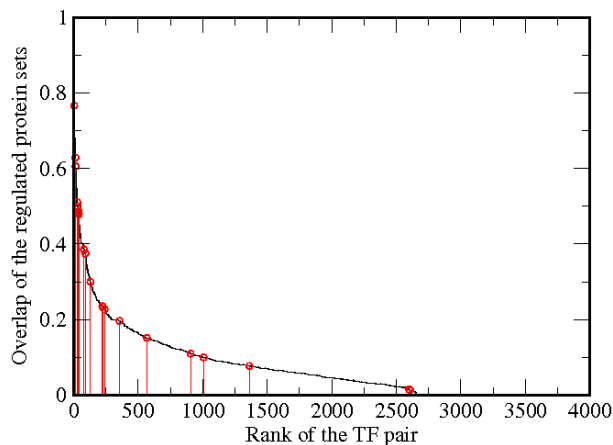


FIG. 10: Correlation between the sets of proteins regulated by the TFs with similar binding motifs. The vertical axis is the percentage overlap of the two sets of genes regulated by an arbitrary pair of TFs, which are ranked on the horizontal axis according to their overlap. The red vertical lines mark those pairs of TFs that are also related by binding motif inclusion. The accumulation of the red lines to the left of the graph is indicative of the correlation described in the text.

On the other hand, the more straightforward expectation that TFs with short binding motifs should regulate more genes is not verified by the same data. This curious fact probably points to certain sequence correlations arising from the duplication and divergence processes [26] that distort the occurrence statistics of the binding motifs in PRs. Note that the result in Fig. 10 is robust to such deviations from the unbiased probabilities for the occurrence of different strings.
